Journal of Organometallic Chemistry, 452 (1993) 151–160

JOM 23401

Structural studies on ruthenium carbonyl hydrides

XVIII *. Synthesis and characterization of $(\mu\text{-H})Ru_3(\mu_3\text{-}\eta^3\text{-XCCRCR'})(CO)_{9-n}(PPh_3)_n$ complexes. Crystal structures of $(\mu\text{-H})Ru_3(\mu_3\text{-}\eta^3\text{-}Et_2NCCHCMe)(CO)_8(PPh_3)$ and $(\mu\text{-H})Ru_3(\mu_3\text{-}\eta^3\text{-MeOCCMeCMe})(CO)_7(PPh_3)_2 \cdot 2CH_2Cl_2$

Melvyn Rowen Churchill, Charles H. Lake, Romana A. Lashewycz-Rubycz [1], Huirong Yao, Robert D. McCargar and Jerome B. Keister *

Department of Chemistry, State University of New York at Buffalo, Buffalo, NY 14214 (USA)

(Received August 20, 1992; in revised form November 10, 1992)

Abstract

Substitution products $HRu_3(\mu_3\text{-}\eta^3\text{-XCCRCR'})(CO)_{9-n}(PPh_3)_n$ (X = OMe, R = R' = Me, n = 1–3; X = OMe, R = H, R' = OEt, n = 2, 3; X = NEt_2, R = H, R' = Me, n = 1, 2) were prepared by using $ONMe_3$-induced ligand substitution. The products were characterized by spectroscopic methods. In addition, $(\mu\text{-H})Ru_3(\mu_3\text{-}\eta^3\text{-}Et_2NCCHCMe)(CO)_8(PPh_3)$ (Mo Kα, 2θ 5.0–50.0°, R_F 5.22% for all 6,374 reflections, 2.62% for those 4,306 reflections with $|F_o| > 6\sigma(|F_o|)$) and $(\mu\text{-H})Ru_3(\mu_3\text{-}\eta^3\text{-MeOCCMeCMe})(CO)_7(PPh_3)_2 \cdot 2CH_2Cl_2$ (Mo Kα, 2θ 8.0–45.0°, R_F 9.52% for all 6,798 reflections, 6.69% for those 3,795 reflections with $|F_o| > 6\sigma(|F_o|)$) were characterized by single-crystal X-ray diffraction. Both compounds crystallize in the triclinic space group $P\bar{1}$, with a 11.277(2) Å, b 11.899(1) Å, c 15.638(2) Å, α = 70.56(1)°, β = 85.23(1)°, γ = 66.00(1)°, V = 1802.8(4) Å^3, and Z = 2 for the former and a = 12.960(2) Å, b = 13.040(2) Å, c = 17.683(3) Å, α = 98.81(1)°, β = 94.50(1)°, γ = 116.50(1)°, V = 2606.2(8) Å^3, and Z = 2 for the latter. In each case the PPh_3 ligands are coordinated *cis* to the bridging hydride and to the sigma Ru–C bond.

1. Introduction

The structures and reaction chemistry of 1,3-dimetalloallyl clusters $HM_3(\mu_3\text{-}\eta^3\text{-XCCRCR'})(CO)_9$, structure **I** (M = Ru or Os, L^1, L^2, L^3 = CO or PPh_3), have been the subjects of many studies in recent years [1–6]. Pi donation from carbon substituents such as dialkylamino or alkoxy into the M_3C_3 cluster core is an important feature in the bonding of these clusters. This conjugation has the structural consequence that, as the pi donor ability of the carbon substituent increases, the cluster core distorts from the *nido* structure (*e.g.* **II**) based upon a pentagonal bipyramid toward an *arachno* structure (*e.g.* **III**) [2].

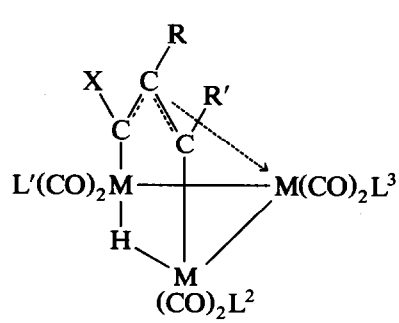

(I)

Correspondence to: Prof. J.B. Keister.

[1] On sabbatical leave from the Department of Chemistry, Hobart & William Smith Colleges, Geneva, NY, USA.

0022-328X/93/$6.00

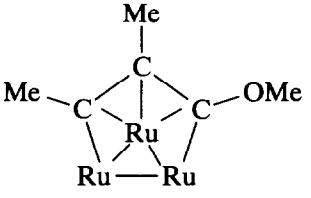

(II)

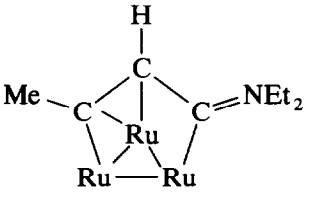

(III)

Substitution of phosphine ligands for carbonyls on transition metal clusters also provides for variation of the steric and electronic properties associated with the cluster core. The mono-substituted clusters $HRu_3(\mu_3\text{-}\eta^3\text{-}C_3H_2Me)(CO)_8(PPh_3)$ and $HRu_3(\mu_3\text{-}\eta^3\text{-}C_3HMe_2)(CO)_8(PPh_3)$ were previously prepared by thermally induced substitution on the parent carbonyls and had been characterized by spectroscopic methods [3]. Substitution was shown to occur on a Ru atom that is bonded to the hydride. However, the coordination site occupied by the PPh_3 ligand could not be unequivocally assigned by spectroscopic methods. To determine the effect of PPh_3 substitution for CO ligands upon the cluster core geometry and to establish the stereochemistry of PPh_3 coordination, we have synthesized *via* trimethylamine-*N*-oxide promoted substitution the clusters $HRu_3(\mu_3\text{-}\eta^3\text{-XCCRCR'})(CO)_{9-n}(PPh_3)_n$ (X = OMe, R = R' = Me, n = 1–3; X = OMe, R = H, R' = OEt, n = 2, 3; X = NEt_2, R = H, R' = Me, n = 1, 2), including the first di- and tri-substituted clusters of the class, and have crystallographically characterized two of these — $(\mu\text{-H})Ru_3(\mu_3\text{-}\eta^3\text{-MeCCHCNEt}_2)(CO)_8(PPh_3)$ and $(\mu\text{-H})Ru_3(\mu_3\text{-}\eta^3\text{-MeCCMeCOMe})(CO)_7(PPh_3)_2$.

2. Experimental section

2.1. General

Infrared spectra were recorded on Mattson Instruments Alpha Centauri FTIR or Beckman 4250 spectrophotometers in cyclohexane or dichloromethane solution. ^1H NMR spectra were obtained on JEOL FX-90, Varian Associates Gemini 300, or Varian Associates VXR-400S instruments, using deuterochloroform as solvent and TMS as reference. ^{31}P NMR spectra were recorded on the VXR-400S instrument in deuterochloroform and chemical shifts are reported relative to *o*-phosphoric acid.

2.2. Starting materials

$HRu_3(\mu_3\text{-}\eta^3\text{-MeOCCMeCMe})(CO)_9$ [4], $HRu_3(\mu_3\text{-}\eta^3\text{-MeOCCHCOEt})(CO)_9$ [4], and $HRu_3(\mu_3\text{-}\eta^3\text{-Et}_2\text{N-CCHCMe})(CO)_9$ [5] were prepared according to reported procedures. Trimethylamine-*N*-oxide dihydrate was obtained from Aldrich.

2.3. $HRu_3(\mu_3\text{-}\eta^3\text{-MeOCCMeCMe})(CO)_{9-n}(PPh_3)_n$ (n = 1, 2)

In a 100 mL Schlenk flask was placed $HRu_3(\mu_3\text{-}\eta^3\text{-MeOCCMeCMe})(CO)_9$ (130 mg, 0.203 mmol) and THF (15 mL) with a magnetic stir bar under nitrogen. To the solution was added a solution of PPh_3 (110 mg, 0.420 mmol) and $ONMe_3 \cdot 2H_2O$ (45 mg, 0.408 mmol) in THF (40 mL). The resulting solution was stirred under nitrogen for 24 h. After evaporation to dryness, the red residue was purified by thin-layer chromatography on silica gel, eluting with cyclohexane : dichloromethane (2:1). Three bands were observed. The top yellow band was a monosubstituted product (isomer **1**) (15.4 mg, 8.4%), the second yellow band was a second monosubstituted product (isomer **2**) (16.4 mg, 9.1%), and the bottom orange band was found to be the disubstituted product (183.0 mg, 80.8%).

$HRu_3(\mu_3\text{-}\eta^3\text{-MeOCCMeCMe})(CO)_8(PPh_3)$. Isomer **1** ($PPh_3$ *cis* to Ru-COMe). ^1H NMR ($CDCl_3$): 7.3 (m, 15H); 3.43 (s, 3H); 2.86 (s, 3H); 2.09 (s, 3H); −19.21 (d, 1H, J(PH) = 17.7 Hz) ppm. ^{31}P NMR ($CDCl_3$): 44.1 ppm. IR (CH_2Cl_2): 2070m, 2029vs, 2011s, 1992m-w, 1973w cm^{-1}. Isomer **2** (PPh_3 *cis* to Ru-CMe). ^1H NMR ($CDCl_3$): 7.3 (m, 15H); 3.88 (s, 3H); 2.20 (d, 3H, J(PH) = 5.2 Hz); 1.96 (s, 3H); −19.05 (d, 1H, J(PH) = 16.4 Hz) ppm. ^{31}P NMR ($CDCl_3$): 45.4 (s, 1P) ppm. IR (CH_2Cl_2): 2073m, 2031vs, 2012s, 1993m-w, 1971w cm^{-1}.

$HRu_3(\mu_3\text{-}\eta^3\text{-MeOCCMeCMe})(CO)_7(PPh_3)_2$. ^1H NMR ($CDCl_3$): 7.1 (m, 30H); 3.45 (s, 3H); 2.20 (s, 3H); 2.15 (d, 3H, J(PH) = 5.5 Hz); −18.06 (t, 1H, J(PH) = 12.5 Hz) ppm. ^{31}P NMR ($CDCl_3$): 51.3 (d, 1P); 44.4 (d, 1P, J(PP) = 8 Hz) ppm. IR (CH_2Cl_2): 2039s, 2002s br, 1962w cm^{-1}. Crystals for analysis were obtained from CH_2Cl_2/hexanes (1:1) and were dried overnight under vacuum. Anal. Found: C, 52.20; H, 3.52. $C_{49}H_{40}O_8P_2Ru_3$ calc.: C, 52.45; H, 3.59.

2.4. $HRu_3(\mu_3\text{-}\eta^3\text{-MeOCCMeCMe})(CO)_6(PPh_3)_3$

In a 100-ml Schlenk flask was added $HRu_3(\mu_3\text{-}\eta^3\text{-MeOCCMeCMe})(CO)_9$ (161 mg, 0.246 mmol) and THF (25 mL) with a magnetic stir bar under nitrogen. To the solution was added a solution of PPh_3 (197 mg, 0.750 mmol) and $ONMe_3 \cdot 2H_2O$ (85 mg, 0.77 mmol) in THF (20 mL). The solution was stirred for three days under nitrogen. After evaporating to dryness, the red residue was purified by thin-layer chromatography on

silica gel eluting with cyclohexane : dichloromethane (2 : 1). Two bands were observed. The top, orange band was the disubstituted product (54.1 mg, 19.7%); the second, red band was found to be the trisubstituted product (132.6 mg, 50.8%).

$HRu_3(\mu_3\text{-}\eta^3\text{-MeOCCMeCMe})(CO)_6(PPh_3)_3$. ^1H NMR ($CDCl_3$): 7.1 (m, 45H); 3.05 (s, 3H); 1.84 (s, 3H); 1.81 (d, 3H, $J(PH) = 4.7$ Hz); and −17.89 (dt, 1H, $J(PH) = 13.3$, 3.5 Hz) ppm. ^{31}P NMR ($CDCl_3$): 48.5 (s, 1P); 42.2 (s, 1P); and 38.6 (s, 1P) ppm. IR (CH_2Cl_2): 2012s, 1987m, 1954m cm^{-1}. Pure samples for analysis were recrystallized from hexanes : dichloromethane (1 : 2). Anal. Found: C, 57.92; H, 4.26. $C_{66}H_{55}O_7P_3Ru_3$ calc.: C, 58.45; H, 4.09.

2.5. $HRu_3(\mu_3\text{-}\eta^3\text{-}Et_2NCCHCMe)(CO)_{9-n}(PPh_3)_n$ (n = 1, 2).

In a 100-ml Schlenk flask was added $HRu_3(\mu_3\text{-}\eta^3\text{-}Et_2NCCHCMe)(CO)_9$ (226 mg, 0.338 mmol) and THF (10 mL) with a magnetic stir bar under nitrogen. To the solution was added PPh_3 (183 mg, 0.699 mmol) and $ONMe_3 \cdot 2H_2O$ (80 mg, 0.717 mmol) in THF (40 mL). The solution was stirred under nitrogen for 24 h. After evaporating to dryness, the orange-yellow residue was purified by thin-layer chromatography, eluting with cyclohexane : dichloromethane (2 : 1). Three bands were observed. The top yellow band was found to be a monosubstituted product (6.4 mg, 2.1%) (isomer **1**). The second yellow band was found to be the second monosubstituted product (25.0 mg, 8.1%) (isomer **2**). The bottom orange yellow band was found to be the disubstituted product (271.1 mg, 70.0%).

$HRu_3(\mu_3\text{-}\eta^3\text{-}Et_2NCCHCMe)(CO)_8(PPh_3)$. Isomer **1** ($PPh_3$ *cis* to Ru-$CNEt_2$). ^1H NMR ($CDCl_3$, 25°C): 7.1 (m, 15H); 5.26 (d, 1 H_a, $J_{ab} = 2.5$ Hz); 4.20 (dq, 1H, $J(HH) = 14.0$, 7.0 Hz); 3.93 (dq, 1H, $J(HH) = 14.0$, 7.0 Hz); 3.83 (dq, 1H, $J(HH) = 14.0$, 7.0 Hz); 3.45 (dq, 1H, $J(HH) = 14.0$, 7.0 Hz); 2.83 (s, 3H); 1.19 (t, 3H, $J(HH) = 7.0$ Hz); 0.78 (t, 3H, $J(HH) = 7.0$ Hz); −17.71 (dd, $1H_b$, $J_{ab} = 2.5$ Hz, $J_{bP} = 19.1$ Hz) ppm. ^{31}P NMR ($CDCl_3$): 35.9 (s, 1P) ppm. IR (CH_2Cl_2): 2064s, 2022vs br, 2002vs br, 1982w, 1960m cm^{-1}.

Isomer **2** (PPh_3 *cis* to Ru-CMe). ^1H NMR ($CDCl_3$, 25°C): 7.1 (m, 15H); 5.86 (d, $1H_a$, $J_{ab} = 2.4$ Hz); 4.21 (dq, 1H, $J(HH) = 14.0$, 7.0 Hz); 3.98 (dq, 1H, $J(HH) = 14.0$, 7.0 Hz); 3.75 (dq, 1H, $J(HH) = 14.0$, 7.0 Hz); 3.58 (dq, 1H, $J(HH) = 14.0$, 7.0 Hz); 2.24 (d, 3H, $J(PH) = 4.3$ Hz); 1.29 (t, 3H, $J(HH) = 7.0$ Hz); 0.91 (t, 3H, $J(HH) = 7.0$ Hz); −17.23 (dd, $1H_b$, $J_{bP} = 17.4$ Hz, $J_{ab} = 2.4$ Hz) ppm. ^{31}P NMR ($CDCl_3$): 45.2 (s, 1P) ppm. IR (CH_2Cl_2): 2062s, 2020vs br, 2001vs br, 1978w, 1953m cm^{-1}.

$HRu_3(\mu_3\text{-}\eta^3\text{-}Et_2NCCHCMe)(CO)_7(PPh_3)_2$. ^1H NMR ($CDCl_3$, 25°C): 7.1 (m, 30H); 6.25 (d, $1H_a$, $J_{ab} = 2.8$ Hz); 4.20 (dq, 1H, $J(HH) = 14.0$, 7.0 Hz); 3.74 (dq, 1H, $J(HH) = 14.0$, 7.0 Hz); 3.52 (dq, 1 H, $J(HH) = 14.0$, 7.0 Hz); 3.28 (dq, 1H, $J(HH) = 14.0$, 7.0 Hz); 2.45 (d, 1H, $J(PH) = 4.5$ Hz); 1.49 (t, 3H, $J(HH) = 7.0$ Hz); 0.79 (t, 3H, $J(HH) = 7.0$ Hz); −16.40 (td, $1H_b$, $J_{bP} = 15.0$, $J_{ab} = 2.8$ Hz) ppm. ^{31}P NMR ($CDCl_3$): 48.2 (s, 1P); 34.6 (s, 1P) ppm. IR (CH_2Cl_2): 2033s, 1992s br, 1950w cm^{-1}. Crystals for analysis were obtained by slow cooling from dichloromethane : hexanes (1 : 1). Anal. Found: C, 53.32; H, 4.02. $C_{51}H_{45}NO_7P_2Ru_3$ calc.: C, 53.31; H, 3.95.

2.6. $HRu_3(\mu_3\text{-}\eta^3\text{-MeOCCHCOEt})(CO)_{9-n}(PPh_3)_n$ (n = 1, 2)

In a 100-mL Schlenk flask was added $HRu_3(\mu_3\text{-}\eta^3\text{-MeOCCHCOEt})(CO)_9$ (100 mg, 0.15 mmol) and THF (15 mL) under nitrogen. To the solution was added PPh_3 (78.6 mg, 0.30 mmol) and $ONMe_3 \cdot 2H_2O$ (33.3 mg, 0.30 mmol) in THF (40 mL). The reaction was stirred under nitrogen for 24 h. After evaporating to dryness, the red residue was purified by thin-layer chromatography on silica gel, eluting with hexane : dichloromethane (1 : 1). Three bands were observed on the plate. The top yellow band consisted of two monosubstituted isomers (31.1 mg, 22.9%). The second orange band consisted of three disubstituted isomers (85.6 mg, 50.7%). The disubstituted isomers were characterized only by the ^1H NMR spectrum of the mixture in $CDCl_3$: isomer **a**, 5.90 (dd, $J = 2.4$, 2.2 Hz) and −18.52 (ddd, $J = 16.8$, 2.2, 2.2 Hz) ppm; isomer **b**, 5.85 (dd, $J = 2.4$, 2.2 Hz) and −18.63 (ddd, $J = 17.6$, 2.2, 2.2 Hz) ppm; isomer **c**, spectrum below; relative ratios after 24 h **a/b/c**, 40/30/25). Only the isomer **c** with two phosphine ligands *cis* to the allyl group was thermodynamically stable. This isomer was obtained after the mixture was stirred under nitrogen in THF or methylene chloride for an additional two days. The third red–orange band was a trisubstituted product (4.9 mg, 2.3%).

$HRu_3(\mu_3\text{-}\eta^3\text{-MeOCCHCOEt})(CO)_7(PPh_3)_2$. IR ($CH_2Cl_2$): 2042s, 2004s, 1967m cm^{-1}. ^1H NMR ($CDCl_3$, 25°C): 7.23 (m, 30H); 3.39 (s, 3H); 3.47 (q, $1H_a$); 3.64 (q, $1H_b$); 1.01 (t, $1H_c$); 6.42 (d, $1H_d$); −17.60 (td, $1H_e$) ppm, $J_{eP} = 11.6$ Hz, $J_{ac} = J_{bc} = 7$ Hz, $J_{de} = 2.4$ Hz. ^{31}P NMR ($CDCl_3$): 43.42 (1P); 42.39 (1P) ppm.

2.7. $HRu_3(\mu_3\text{-}\eta^3\text{-MeOCCHCOEt})(CO)_6(PPh_3)_3$

In a 100-mL Schlenk flask was added $HRu_3(\mu_3\text{-}\eta^3\text{-MeOCCHCOEt})(CO)_9$ (100 mg, 0.15 mmol) and THF (15 mL) under nitrogen. To the solution was added PPh_3 (117 mg, 0.45 mmol) and $ONMe_3 \cdot 2H_2O$ (50 mg, 0.45 mmol) in THF (40 mL). The reaction was stirred under nitrogen for two days. After evaporating to dry-

TABLE 1. X-ray diffraction data for $(\mu\text{-H})Ru_3(\mu_3\text{-}\eta^3\text{-}Et_2NCCHCMe)(CO)_8(PPh_3)$ and $(\mu\text{-H})Ru_3(\mu_3\text{-}\eta^3\text{-MeOCCMeCMe})(CO)_7(PPh_3)_2 \cdot 2CH_2Cl_2$

	$Ru_3(Et_2NCCHCMe)(PPh_3)$ complex	$Ru_3(MeOCCMeCMe)(PPh_3)_2$ complex
(A) Crystal data		
Empirical formula	$C_{34}H_{30}NO_8PRu_3$	$C_{49}H_{40}O_8P_2Ru_3 \cdot 2CH_2Cl_2$
Color; Habit	orange	orange, platelike crystal
Crystal size (mm)	$0.2 \times 0.2 \times 0.25$	$0.23 \times 0.20 \times \sim 0.1$
Crystal system	Triclinic	Triclinic
Space group	$P\bar{1}$	$P\bar{1}$
Unit cell dimensions	$a = 11.277(2)$ Å	$a = 12.960(2)$ Å
	$b = 11.889(1)$ Å	$b = 13.040(2)$ Å
	$c = 15.638(2)$ Å	$c = 17.683(3)$ Å
	$\alpha = 70.56(1)°$	$\alpha = 98.81(1)°$
	$\beta = 85.23(1)°$	$\beta = 94.50(1)°$
	$\gamma = 66.00(1)°$	$\gamma = 116.50(1)°$
Volume	1802.8(4) Å^3	2606.2(8) Å^3
Z	2	2
Formula weight	914.9	1291.9
Density (calc.)	1.685 Mg m^{-3}	1.646 Mg m^{-3}
Absorption coefficient	1.308 mm^{-1}	1.162 mm^{-1}
$F(000)$	904	1288
(B) Data collection		
Diffractometer used	Siemens R3m/V	[a]
Radiation	Mo-Kα ($\lambda = 0.71073$ Å)	[a]
Temperature (K)	298	295
Monochromator	Highly oriented graphite crystal	[a]
2θ Range	5.0 to 50.0°	8.0 to 45.0°
Scan type	2θ–θ	[a]
Scan speed	Constant; 1.00° min^{-1} in ω	Constant; 1.50°/min. in ω
Scan range (ω)	0.55° plus Kα-separation	0.60° plus Kα-separation
Background measurement	Stationary crystal and stationary counter at beginning and end of scan, each for 25.0% of total scan time	[a]
Standard reflections	3 measured every 97 reflections	[a]
Index ranges	$0 \le h \le 13$, $-12 \le k \le 14$, $-18 \le l \le 18$	$-13 \le h \le 12$, $0 \le k \le 14$, $-19 \le l \le 18$
Reflections collected	6767	7150
Independent reflections	6374 ($R_{int} = 0.84\%$)	6798 ($R_{int} = 1.60\%$)
Reflections ($F > 6.0\sigma(F)$)	4306	3795
Absorption correction	Semi-empirical	Semi-empirical
Min./Max. transmission	0.6708/0.7153	0.8004/0.9776
(C) Solution and refinement		
System used	Siemens SHELXTL PLUS (VMS)	[a]
Solution	Direct methods	[a]
Refinement method	Full-matrix least-squares	[a]
Quantity minimized	$\Sigma w(F_o - F_c)^2$	[a]
Extinction correction	$\chi = 0.00002(3)$ [where $F^* = F[1 + 0.002\chi F^2/\sin(2\theta)]^{-1/4}$]	$\chi = 0.0003(2)$
Organic hydrogen atoms	Riding model, fixed isotropic U	[a]
Weighing scheme	$w^{-1} = \sigma^2(F) + 0.0005F^2$	$w^{-1} = \sigma^2(F) + 0.0020F^2$
Number of parameters refined	429	389
Final R indices (data $> 6\sigma$)	$R = 2.62\%$, $Rw = 2.64\%$	$R = 6.69\%$, $Rw = 9.34\%$
R Indices (all data)	$R = 5.22\%$, $Rw = 3.76\%$	$R = 9.52\%$, $Rw = 9.89\%$
Goodness-of-fit	0.91	1.58
Data-to-parameter ratio	14.9:1	9.8:1
Largest difference peak	0.58 eÅ^{-3}	1.50 eÅ^{-3}
Largest difference hole	-0.58 eÅ^{-3}	-0.96 eÅ^{-3}

[a] Entry as for previous column.

ness, the red residue was purified by thin-layer chromatography on silica gel, eluting with hexane : dichloromethane solution (2 : 1). Two bands were observed on the plate. The first orange band was the disubstituted product (60.8 mg, 35.6%). The second red band was the trisubstituted product (59.2 mg, 28.8%).

$HRu_3(\mu_3\text{-}\eta^2\text{-MeOCCHCOEt})(CO)_6(PPh_3)_3$. IR ($CH_2Cl_2$): 2017s, 1996m, 1955m cm^{-1}. ^1H NMR ($CDCl_3$, 25°C): 7.3 (m, 45H); 6.12 (dd, $1H_a$, $J_{aP} = 6.0$ Hz, $J_{ab} = 2.4$ Hz); 2.87 (s, 3H); 2.87 (q, 1H, $J(HH) = 7$ Hz); 2.80 (q, 1H, $J(HH) = 7$ Hz); 0.80 (t, 3H, $J(HH) = 7$ Hz), −17.20 (br t, $1H_b$, $J_{bP} = 12.6$ Hz) ppm. ^{31}P NMR ($CDCl_3$): 40.29 (s, 1P); 38.55 (s, 1P); 34.47 (s, 1P) ppm.

2.8. Collection of X-ray diffraction data for $(\mu\text{-H})Ru_3(\mu_3\text{-}\eta^3\text{-}Et_2NCCHCMe)(CO)_8(PPh_3)$

A well-formed orange crystal of dimensions 0.2 × 0.2 × 0.25 mm was sealed into a thin-walled capillary and mounted on a Siemens R3m/V four-circle single-crystal diffractometer. Determination of the orientation matrix and unit cell parameters were carried out as described previously [7]; details of data collection are outlined in Table 1. All data were corrected for the effects of absorption and for Lorentz and polarization factors. The crystal belongs to the triclinic system. Intensity statistics and the far greater probability of a synthetic crystal with $Z = 2$ belonging to the centrosymmetric space group [8] each suggested the space group $P\bar{1}$ (C_i^1; No. 2). This was confirmed by the successful solution of the structure in this centrosymmetric space group.

2.9. Solution and refinement of the structure of $(\mu\text{-H})Ru_3(\mu_3\text{-}\eta^3\text{-}Et_2NCCHCMe)(CO)_8(PPh_3)$

Crystallographic calculations were carried out on a VAX3100 workstation, with use of the Siemens SHELXTL PLUS program set [9]. Analytical scattering factors for neutral atoms were corrected for the $\Delta f'$ and $i\Delta f''$ components of anomalous dispersion. The structure was solved by direct methods and was refined to convergence with $R = 5.22\%$ and $Rw = 3.76\%$ for all 6,374 independent reflections (Mo-Kα radiation, $2\theta = 5.0$–$50.0°$) and $R = 2.62\%$ and $Rw = 2.64\%$ for those 4,306 reflections with $|F_o| > 6\sigma(|F_o|)$. All organic hydrogen atoms were included in idealized positions based upon C–H(X-ray) = 0.96 Å [10] and with their U values set equal to the U_{eq} values of their attached carbon atoms. (The hydridic hydrogen atom H(1) was subjected to refinement.) A minor correction was made for the effects of secondary extinction (see Table 1). A final difference-Fourier map showed features in the range $-0.58 \rightarrow +0.58$ e$^-$ Å^{-3} ($-0.30 \rightarrow +0.30$ e$^-$ Å^{-3} for data with $|F_o| > 6\sigma(F_o)$). Final atomic coordinates are collected in Table 2.

TABLE 2. Final atomic coordinates (×10^4) and equivalent isotropic displacement coefficients (Å^2 ×10^3) for $(\mu\text{-H})Ru_3(\mu_3\text{-}\eta^3\text{-}Et_2NCCHCMe)(CO)_8(PPh_3)$

	x	y	z	U_{eq} [a]
Ru(1)	1584(1)	2762(1)	2516(1)	31(1)
Ru(2)	3031(1)	4440(1)	1745(1)	34(1)
Ru(3)	1990(1)	4185(1)	3451(1)	34(1)
H(1)	2830(37)	3009(36)	1817(25)	37(11)
P(1)	2332(1)	918(1)	2074(1)	33(1)
N(1)	5674(3)	2983(3)	2867(2)	40(2)
O(11)	−403(4)	2146(5)	3779(3)	81(2)
O(12)	−663(4)	4410(4)	1061(3)	76(2)
O(21)	4532(5)	3884(4)	114(3)	83(3)
O(22)	587(4)	6549(4)	568(3)	87(2)
O(23)	3656(5)	6655(4)	1816(3)	89(3)
O(31)	760(4)	3448(4)	5231(3)	73(2)
O(32)	−662(4)	6148(4)	2543(3)	77(2)
O(33)	2951(5)	5894(4)	4022(3)	90(3)
C(1)	4440(4)	3144(4)	2806(3)	34(2)
C(2)	3945(4)	2466(4)	3601(3)	34(2)
C(3)	2932(4)	2070(4)	3594(3)	32(2)
C(4)	2952(5)	977(4)	4466(3)	43(2)
C(5)	6560(5)	2171(5)	3686(3)	53(2)
C(6)	6463(6)	2899(7)	4330(4)	79(4)
C(7)	6315(5)	3607(5)	2103(3)	54(3)
C(8)	7218(6)	2636(7)	1660(4)	88(4)
C(11)	372(5)	2350(5)	3294(3)	50(2)
C(12)	200(5)	3797(5)	1578(3)	47(2)
C(21)	3984(5)	4087(5)	724(3)	52(3)
C(22)	1465(5)	5727(5)	1009(3)	52(2)
C(23)	3413(5)	5830(5)	1793(3)	52(2)
C(31)	1252(5)	3713(5)	4573(3)	47(2)
C(32)	352(6)	5406(5)	2850(3)	54(3)
C(33)	2587(5)	5277(5)	3787(3)	52(3)
C(41)	2713(4)	1073(4)	892(3)	40(2)
C(42)	2439(5)	2276(5)	234(3)	49(2)
C(43)	2720(6)	2375(6)	−654(3)	70(3)
C(44)	3256(6)	1272(7)	−896(4)	80(4)
C(45)	3531(6)	78(7)	−258(4)	76(4)
C(46)	3285(5)	−34(5)	634(3)	56(3)
C(51)	3876(4)	−373(4)	2658(3)	38(2)
C(52)	4886(4)	−11(5)	2708(3)	51(2)
C(53)	6065(5)	−937(7)	3127(4)	70(3)
C(54)	6267(6)	−2216(7)	3499(4)	82(4)
C(55)	5285(7)	−2579(6)	3452(4)	80(3)
C(56)	4091(5)	−1677(5)	3037(3)	58(3)
C(61)	1220(5)	95(5)	2277(4)	50(2)
C(62)	615(5)	33(6)	1588(5)	76(4)
C(63)	−233(7)	−629(9)	1791(8)	119(6)
C(64)	−426(8)	−1164(9)	2679(10)	140(8)
C(65)	141(8)	−1085(7)	3373(8)	118(5)
C(66)	970(6)	−456(5)	3167(5)	75(3)

[a] Equivalent isotropic U defined as one third of the trace of the orthogonalized U_{ij} tensor.

2.10. Collection of X-ray diffraction data for $(\mu\text{-H})Ru_3(\mu_3\text{-}\eta^3\text{-MeOCCMeCMe})(CO)_7(PPh_3)_2 \cdot 2CH_2Cl_2$

Crystals of this material tended to be rather plate-like and of poor quality. The crystal selected for the X-ray diffraction study had dimensions of 0.23 × 0.20 × ~0.1 mm. It was sealed into a capillary and data

TABLE 3. Interatomic distances, in Å, for $(\mu\text{-H})Ru_3(\mu_3\text{-}\eta^3\text{-}Et_2NCCHCMe)(CO)_8(PPh_3)$

Ru(1)–Ru(2)	2.969(1)	Ru(1)–Ru(3)	2.757(1)
Ru(1)–H(1)	1.768(40)	Ru(1)–P(1)	2.325(1)
Ru(1)–C(3)	2.076(4)	Ru(1)–C(11)	1.859(5)
Ru(1)–C(12)	1.928(5)	Ru(2)–Ru(3)	2.796(1)
Ru(2)–H(1)	1.773(49)	Ru(2)–C(1)	2.097(4)
Ru(2)–C(21)	1.918(5)	Ru(2)–C(22)	1.938(5)
Ru(2)–C(23)	1.894(7)	Ru(3)–C(2)	2.279(4)
Ru(3)–C(3)	2.236(4)	Ru(3)–C(31)	1.888(5)
Ru(3)–C(32)	1.898(5)	Ru(3)–C(33)	1.908(7)
P(1)–C(41)	1.827(5)	P(1)–C(51)	1.839(4)
P(1)–C(61)	1.831(6)	N(1)–C(1)	1.332(6)
N(1)–C(5)	1.475(6)	N(1)–C(7)	1.484(6)
O(11)–C(11)	1.156(7)	O(12)–C(12)	1.138(6)
O(21)–C(21)	1.132(7)	O(22)–C(22)	1.134(6)
O(23)–C(23)	1.133(9)	O(31)–C(31)	1.139(6)
O(32)–C(32)	1.142(6)	O(33)–C(33)	1.136(10)
C(1)–C(2)	1.446(6)	C(2)–C(3)	1.404(8)
C(3)–C(4)	1.533(5)	C(5)–C(6)	1.503(10)
C(7)–C(8)	1.518(9)	C(41)–C(42)	1.383(6)
C(41)–C(46)	1.391(8)	C(42)–C(43)	1.376(7)
C(43)–C(44)	1.369(11)	C(44)–C(45)	1.364(9)
C(45)–C(46)	1.371(8)	C(51)–C(52)	1.388(9)
C(51)–C(56)	1.386(7)	C(52)–C(53)	1.372(6)
C(53)–C(54)	1.362(11)	C(54)–C(55)	1.357(13)
C(55)–C(56)	1.376(7)	C(61)–C(62)	1.359(11)
C(61)–C(66)	1.387(9)	C(62)–C(63)	1.425(13)
C(63)–C(64)	1.363(17)	C(64)–C(65)	1.350(20)
C(65)–C(66)	1.377(12)		

were treated as described for the previous study. This crystal also belongs to space group $P\bar{1}$ (C_i^1; No. 2).

2.11. Solution and refinement of the structure of $(\mu\text{-H})Ru_3(\mu_3\text{-}\eta^3\text{-MeOCCMeCMe})(CO)_7(PPh_3)_2 \cdot 2CH_2Cl_2$

This was carried out as described above. Because of the weak diffracting characteristics of the crystal, data were collected only to $2\theta = 45°$ (Mo-Kα). Refinement converged with $R = 6.69\%$ and $Rw = 9.34\%$ for those 3,795 data with $|F_o| > 6\sigma(|F_o|)$ and $R = 9.52\%$ and $Rw = 9.89\%$ for all 6,798 data. We attribute these rather high values to the following: (a) the weakness of the data (only 55.8% is greater than 6σ) and (b) large amplitudes of "thermal motion" for the two independent CH_2Cl_2 molecules of solvation. All hydrogen atoms were included in calculated positions. A final difference-Fourier map showed features in the range $-0.96 \rightarrow +1.50$ e$^-$ Å^{-3}, with all major features being in close proximity either to the ruthenium atoms or to the chlorine atoms of the CH_2Cl_2 molecules. Final atomic parameters are compiled in Table 4.

3. Results and discussion

3.1. Syntheses and spectroscopic characterizations

The use of trimethylamine-*N*-oxide to induce selective substitutions for carbonyl ligands under mild conditions is well-known [11]. Application of this method allows up to one substitution per metal atom, with little selectivity with regard to the particular metal of the cluster on which substitution occurs. The regiochemistry is easily established by spectroscopic methods (*vide infra*). The two monosubstituted isomers having PPh_3 coordinated to hydride-bridged Ru atoms are formed in similar amounts. Disubstitution on $HRu_3(\mu_3\text{-}\eta^3\text{-MeOCCHCOEt})(CO)_9$ produces comparable quantities of each of the three possible regioisomers (structure **I**: isomer **1**, $L^1 = L^3 = PPh_3$, $L^2 = CO$; isomer **2**, $L^2 = L^3 = PPh_3$, $L^1 = CO$; isomer **3**, $L^1 = L^2 = PPh_3$, $L^3 = CO$) within 24 h; however, in solution over a further two day period isomers **1** and **2**, each having one PPh_3 ligand on a hydride-bridged Ru atom and one PPh_3 ligand on the Ru atom that is η^3-bonded to the MeOCCHCOEt ligand, convert to the thermodynamically favored isomer **3** with each phosphine on one of the hydride-bridged Ru atoms. In all other derivatives $HRu_3(\mu_3\text{-}\eta^3\text{-XCCRCR'})(CO)_{9-n}L_n$, $n = 1$ or 2, the only products are substituted on the hydride-bridged Ru atoms, so the distinction between kinetic and thermodynamic determination of regiochemistry cannot be made. A previous study of thermally induced substitution on $HRu_3(\mu_3\text{-}\eta^3\text{-}C_3H_2Me)(CO)_9$ and $HRu_3(\mu_3\text{-}\eta^3\text{-}C_3HMe_2)(CO)_9$ found monosubstitution only on Ru atoms bridged by the hydride [3].

Spectroscopic characterizations (see Experimental section) are straightforward. It was previously established that PR_3 substitution on a Ru atom bridged by the hydride ligand gave rise to a hydride–phosphorus coupling constant of about 12 Hz and ^4J(P–H) of about 4 Hz to the C–CH_3 groups [3]. Thus, the ^{1}H NMR spectra allow clear differentiation between the various mono- and di-substituted isomers distinguished by the regiochemistry of substitution. However, spectroscopic methods did not allow for determination of stereochemistry of the products; therefore, single-crystal X-ray diffraction studies were undertaken.

3.2. Description of the molecular structure of $(\mu\text{-H})Ru_3(\mu_3\text{-}\eta^3\text{-}Et_2NCCHCMe)(CO)_8(PPh_3)$

The crystal consists of an ordered racemic array of the two enantiomers of the chiral cluster molecules. There are no abnormally short intermolecular contacts. The molecular geometry and labelling of essential atoms are shown in Fig. 1. Interatomic distances are collected in Table 3. Items of particular interest are as follows.

(1) The three ruthenium atoms are arranged in a triangle with the hydrido-bridged distance being Ru(1)–Ru(2) = 2.969(1) Å as compared to Ru(1)–Ru(3) = 2.757(1) Å and Ru(2)–Ru(3) = 2.796(1) Å.

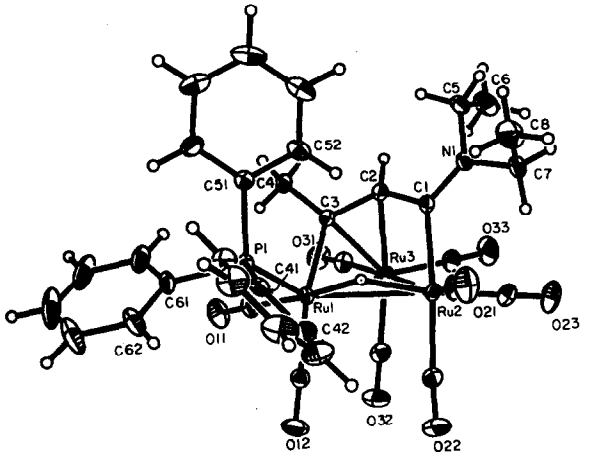

Fig. 1. Overall molecular structure and atomic labelling for $(\mu\text{-H})Ru_3(\mu_3\text{-}\eta^3\text{-}Et_2NCCHCMe)(CO)_8(PPh_3)$.

These distances may be compared with distances of 2.8512(4)–2.8595(4) Å (average = 2.853 Å in $Ru_3(CO)_{12}$ [12] and with values of Ru–(H)–Ru = 2.968(1) Å and Ru–Ru = 2.750(1) Å and 2.781(1) Å in the closely related species $(\mu\text{-H})Ru_3(\mu_3\text{-}\eta^3\text{-}Me_2NCCHCMe)(CO)_9$ [6].

(2) The $Et_2NCCHCMe$ ligand is linked to the triruthenium cluster in a $\mu_3\text{-}\eta^3$ mode yielding the arachno structure (III) for the Ru_3C_3 moiety. Thus the terminal carbon atoms are associated with the σ-bonded distances Ru(1)–C(3) = 2.076(4) Å and Ru(2)–C(1) = 2.097(4) Å. Atom Ru(3) is associated with metal–carbon distances of Ru(3) ··· C(1) = 2.788(4) Å, Ru(3)–C(2) = 2.279(4) Å and Ru(3)–C(3) = 2.236(4) Å. We note here that distances in $(\mu\text{-H})Ru_3(\mu_3\text{-}\eta^3\text{-}Me_2NCCHCMe)(CO)_9$ [6] are 2.061(6) Å and 2.095(6) Å for the Ru–C σ-bonds and (sequentially) Ru ··· C = 2.689(6) Å, Ru–C = 2.296(5) Å and Ru–C = 2.248(5) Å for the delocalized Ru-ligand interaction. Thus the presence of the PPh_3 ligand in the present molecule acts to enhance the η^2-bonding (as opposed to η^3-bonding) at Ru(3).

Distances along the backbone of the all-*trans* system C(7)–N(1)–C(1)–C(2)–C(3)–C(4) are C(7)–N(1) = 1.484(6) Å, N(1)–C(1) = 1.332(6) Å, C(1)–C(2) = 1.446(6), C(2)–C(3) = 1.404(8) Å and C(3)–C(4) = 1.533(5) Å. Angles of interest are N(1)–C(1)–C(2) = 117.3(3)°, C(1)–C(2)–C(3) = 125.3(4) and C(2)–C(3)–C(4) = 112.7(4)°.

(3) The PPh_3 ligand occupies an equatorial site on Ru(1), *cis* to the bridging hydride and to the sigma Ru–C(allyl) bond, with Ru(1)–P(1) = 2.325(1) Å.

(4) The μ-hydride ligand defined by H(1) (that was both located and refined) spans Ru(1) and Ru(2) in an equatorial position with Ru(1)–H(1) = 1.77(4) Å,

TABLE 4. Final atomic coordinates ($\times 10^4$) and equivalent isotropic displacement coefficients ($Å^2 \times 10^3$) for $(\mu\text{-H})Ru_3(\mu_3\text{-}\eta^3\text{-MeOCC-MeCMe})(CO)_7(PPh_3)_2 \cdot 2CH_2Cl_2$

	x	y	z	U_{eq} [a]
Ru(1)	3150(1)	2645(1)	3474(1)	42(1)
Ru(2)	3562(1)	2970(1)	1883(1)	46(1)
Ru(3)	1750(1)	3198(1)	2511(1)	54(1)
P(1)	3865(3)	1547(4)	4084(2)	41(2)
P(2)	4165(4)	1778(4)	1106(2)	47(2)
C(1)	1182(16)	1497(16)	729(10)	65(5)
C(2)	1730(14)	1820(15)	1576(9)	52(4)
C(3)	1017(13)	1194(13)	2072(8)	38(4)
C(3A)	−249(15)	244(16)	1767(10)	65(5)
C(4)	1482(13)	1433(13)	2902(9)	43(4)
O(5)	593(10)	763(10)	3268(7)	65(3)
C(6)	633(17)	867(17)	4063(10)	74(6)
C(11)	2641(15)	3194(17)	4334(11)	62(10)
O(11)	2357(12)	3592(13)	4819(8)	88(8)
C(12)	4601(17)	4008(17)	3833(10)	62(10)
O(12)	5425(12)	4882(12)	4103(8)	81(7)
C(21)	5080(19)	4226(17)	2274(10)	60(11)
O(21)	6021(13)	4998(13)	2487(8)	93(8)
C(22)	3529(18)	3810(17)	1201(14)	85(12)
O(22)	3455(17)	4391(14)	710(10)	114(11)
C(31)	3082(17)	4675(20)	2886(10)	66(11)
O(31)	3751(15)	5626(13)	3098(9)	95(9)
C(32)	748(18)	3318(19)	3211(12)	78(12)
O(32)	118(13)	3367(17)	3608(11)	127(12)
C(33)	1058(18)	3679(19)	1741(14)	90(13)
O(33)	715(18)	4006(17)	1280(11)	139(13)
C(41)	5467(13)	2285(13)	4351(9)	42(4)
C(42)	6014(17)	2432(16)	5093(11)	68(5)
C(43)	7193(18)	3016(18)	5279(12)	82(6)
C(44)	7856(18)	3496(17)	4758(11)	71(5)
C(45)	7372(16)	3331(16)	4005(11)	67(5)
C(46)	6143(14)	2736(14)	3813(9)	47(4)
C(51)	3389(14)	1224(14)	5013(9)	47(4)
C(52)	2875(14)	89(15)	5147(9)	52(4)
C(53)	2552(16)	−78(17)	5875(10)	66(5)
C(54)	2676(16)	838(17)	6411(11)	66(5)
C(55)	3180(14)	1919(16)	6282(10)	56(5)
C(56)	3534(13)	2141(14)	5584(9)	47(4)
C(61)	3564(13)	86(13)	3542(8)	42(4)
C(62)	4402(15)	−296(15)	3492(9)	54(4)
C(63)	4080(16)	−1406(16)	3134(10)	61(5)
C(64)	2957(18)	−2144(19)	2797(11)	77(6)
C(65)	2115(16)	−1835(16)	2838(10)	62(5)
C(66)	2422(14)	−693(14)	3195(9)	50(4)
C(71)	5394(13)	1618(13)	1560(8)	42(4)
C(72)	5301(14)	561(15)	1682(9)	49(4)
C(73)	6260(16)	516(17)	2021(10)	65(5)
C(74)	7338(18)	1486(17)	2216(11)	74(6)
C(75)	7459(17)	2554(18)	2123(10)	68(5)
C(76)	6480(14)	2618(16)	1789(9)	57(5)
C(81)	4625(16)	2176(16)	191(10)	62(5)
C(82)	5667(15)	2287(15)	−29(10)	61(5)
C(83)	5974(18)	2597(17)	−735(11)	73(6)
C(84)	5258(19)	2776(19)	−1212(13)	89(7)
C(85)	4205(19)	2666(19)	−1030(12)	87(6)
C(86)	3893(17)	2390(17)	−315(11)	71(5)
C(91)	3056(12)	265(13)	756(8)	39(4)
C(92)	2362(14)	−322(14)	1290(9)	49(4)

TABLE 4 (continued)

	x	y	z	U_{eq} [a]
C(93)	1442(15)	−1462(16)	1040(10)	62(5)
C(94)	1298(15)	−2040(16)	278(9)	56(5)
C(95)	1941(15)	−1497(15)	−238(10)	58(5)
C(96)	2828(16)	−344(16)	−5(10)	62(5)
C(1S)	7972(31)	5448(34)	821(20)	163(12)
C(2S)	8810(32)	6350(34)	3621(20)	162(12)
C1(1S)	8347(10)	6824(12)	1251(10)	260(11)
C1(2S)	8964(10)	5042(9)	903(7)	184(7)
C1(3S)	9652(11)	5678(9)	3280(9)	251(9)
C1(4S)	9736(15)	7663(12)	3993(13)	395(15)

[a] Equivalent isotropic U defined as one third of the trace of the orthogonalized U_{ij} tensor.

Ru(2)–H(1) = 1.77(5) and Ru(1)–H(1)–Ru(2) = 114(2)°.

(5) Individual Ru–CO bond lengths range from 1.859(5) Å to 1.938(5) Å. Each carbonyl ligand is in a unique environment as a result of the low symmetry (C_1) of the molecule as a whole and of the $(\mu\text{-H})Ru_3(\mu_3\text{-}\eta^3\text{-}C_3)(CO)_8$ moiety (see Fig. 2). Two of the shorter Ru–CO bonds are those *trans* to the μ-hydride ligand, with Ru(1)–C(11) = 1.859(5) Å and Ru(2)–C(23) = 1.894(7) Å. [Note that H(1)–Ru(1)–C(11) = 175.0(11)° and H(1)–Ru(2)–C(23) = 172.6(11)°.] Carbonyl ligands *trans* to the terminal, σ-bonded, carbon atoms of the $Et_2NCCHCMe$ ligand are the two longest. Thus, Ru(2)–C(22) = 1.938(5) Å with C(1)–Ru(2)–C(22) = 165.8(2)° and Ru(1)–C(12) = 1.928(5) Å with C(3)–Ru(1)–C(12) = 166.0(2)°.

3.3. Description of the structure of $(\mu\text{-H})Ru_3(\mu_3\text{-}\eta^3\text{-MeOCCMeCMe})(CO)_7(PPh_3)_2 \cdot 2CH_2Cl_2$

The crystal contains ruthenium cluster molecules and dichloromethane of solvation in a 1:2 ratio. As

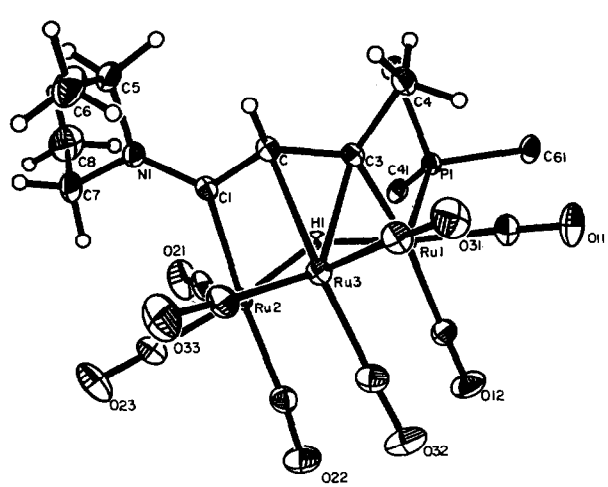

Fig. 2. Molecular core of $(\mu\text{-H})Ru_3(\mu_3\text{-}\eta^3\text{-}Et_2NCCHCMe)(CO)_8(PPh_3)$.

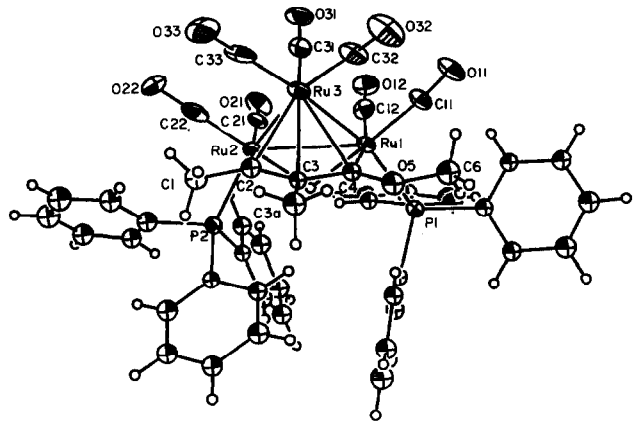

Fig. 3. Molecular structure and atomic labelling for $(\mu\text{-H})Ru_3(\mu_3\text{-}\eta^3\text{-MeOCCMeCMe})(CO)_7(PPh_3)_2$.

with the previous structure, the individual cluster molecules are chiral, but the crystal contains an ordered racemic array of the two enantiomeric forms. The overall molecular geometry is illustrated in Fig. 3. Interatomic distances are collected in Table 5. It should be emphasized that this crystallographic study is of limited precision, as a result (in part) of the presence of two CH_2Cl_2 molecules of solvation. (Compare our structural studies of $(\mu\text{-H})_3Ru_3(\mu_3\text{-COMe})(CO)_6\{\mu_3\text{-}(PPh_2CH_2)_3CMe\}$ and $(\mu\text{-H})_3Ru_3(\mu_3\text{-COMe})(CO)_7\{\mu_2\text{-}(PPh_2)_3CH\} \cdot 1.25\ CH_2Cl_2$, where the presence of CH_2Cl_2 also caused problems [13].)

Interesting points on the current structure are as follows.

(1) The overall molecular structure of $(\mu\text{-H})Ru_3(\mu_3\text{-}\eta^3\text{-MeOCCMeCMe})(CO)_7(PPh_3)_2$ is similar to that of its parent compound $(\mu\text{-H})Ru_3(\mu_3\text{-}\eta^3\text{-MeOCCMeCMe})(CO)_9$ [2] with the Ru_3C_3 center closer to having the *closo* system (II) than the arachno system of the structure reported above.

(2) The hydrido-bridged ruthenium–ruthenium bond, Ru(1)–Ru(2) = 2.966(2) Å, is substantially longer than the other two intermetallic distances, Ru(1)–Ru(3) = 2.787(2) Å and Ru(2)–Ru(3) = 2.789(2) Å. For comparison, distances in $(\mu\text{-H})Ru_3(\mu_3\text{-}\eta^3\text{-MeOCCMeCMe})(CO)_9$ are Ru(H)–Ru = 2.919(1) Å and Ru–Ru = 2.756(1) Å and 2.774(1) Å [2].

(3) The MeOCCMeCMe ligand is bound in a $\mu_3\text{-}\eta^3$ mode to the triruthenium cluster. The terminal carbon atoms are linked to ruthenium atoms with Ru(2)–C(2) = 2.131(11) Å and Ru(1)–C(4) = 2.072(10) Å (*cf.* 2.085(5) Å and 2.060(5) Å for $(\mu\text{-H})Ru_3(\mu_3\text{-}\eta^3\text{-MeOCCMeCMe})(CO)_9$ [2]). The remaining ruthenium atom binds somewhat asymmetrically to all three carbon atoms of the allyl system, with Ru(3)–C(2) = 2.219(14) Å, Ru(3)–C(3) = 2.297(12) Å and Ru(3)–C(4) = 2.387(14) Å (*cf.* values of 2.238(5), 2.304(5) and 2.433(5)

TABLE 5. Interatomic distances, in Å, for $(\mu\text{-H})Ru_3(\mu_3\text{-}\eta^3\text{-MeOC-CMeCMe})(CO)_7(PPh_3)_2\cdot 2CH_2Cl_2$

Ru(1)–Ru(2)	2.964(2)	Ru(1)–Ru(3)	2.787(2)
Ru(1)–P(1)	2.361(6)	Ru(1)–C(4)	2.076(13)
Ru(1)–C(11)	1.872(21)	Ru(1)–C(12)	1.893(15)
Ru(2)–Ru(3)	2.788(2)	Ru(2)–P(2)	2.348(6)
Ru(2)–C(2)	2.134(15)	Ru(2)–C(21)	1.896(17)
Ru(2)–C(22)	1.759(26)	Ru(3)–C(2)	2.236(18)
Ru(3)–C(3)	2.319(15)	Ru(3)–C(4)	2.390(18)
Ru(3)–C(31)	1.895(17)	Ru(3)–C(32)	1.902(25)
Ru(3)–C(33)	1.903(27)	P(1)–C(41)	1.840(15)
P(1)–C(51)	1.844(17)	P(1)–C(61)	1.849(17)
P(2)–C(71)	1.835(19)	P(2)–C(81)	1.837(19)
P(2)–C(91)	1.815(13)	C(1)–C(2)	1.517(23)
C(2)–C(3)	1.400(22)	C(3)–C(3A)	1.536(19)
C(3)–C(4)	1.473(20)	C(4)–O(5)	1.379(19)
O(5)–C(6)	1.385(22)	C(11)–O(11)	1.107(27)
C(12)–O(12)	1.155(19)	C(21)–O(21)	1.166(22)
C(22)–O(22)	1.261(33)	C(31)–O(31)	1.130(23)
C(32)–O(32)	1.134(31)	C(33)–O(33)	1.124(36)
C(41)–C(42)	1.384(24)	C(41)–C(46)	1.364(23)
C(42)–C(43)	1.353(28)	C(43)–C(44)	1.341(30)
C(44)–C(45)	1.369(27)	C(45)–C(46)	1.409(24)
C(51)–C(52)	1.393(25)	C(51)–C(56)	1.373(24)
C(52)–C(53)	1.403(25)	C(53)–C(54)	1.344(29)
C(54)–C(55)	1.329(27)	C(55)–C(56)	1.378(24)
C(61)–C(62)	1.385(30)	C(61)–C(66)	1.387(19)
C(62)–C(63)	1.345(26)	C(63)–C(64)	1.355(24)
C(64)–C(65)	1.324(37)	C(65)–C(66)	1.385(26)
C(71)–C(72)	1.381(27)	C(71)–C(76)	1.398(18)
C(72)–C(73)	1.367(30)	C(73)–C(74)	1.373(22)
C(74)–C(75)	1.368(34)	C(75)–C(76)	1.398(32)
C(81)–C(82)	1.387(30)	C(81)–C(86)	1.399(32)
C(82)–C(83)	1.404(27)	C(83)–C(84)	1.326(36)
C(84)–C(85)	1.377(37)	C(85)–C(86)	1.408(30)
C(91)–C(92)	1.424(22)	C(91)–C(96)	1.388(22)
C(92)–C(93)	1.400(20)	C(93)–C(94)	1.393(24)
C(94)–C(95)	1.349(25)	C(95)–C(96)	1.394(21)
C(1S)–C1(1S)	1.667(44)	C(1S)–C1(2S)	1.599(51)
C(2S)–C1(3S)	1.766(51)	C(2S)–C1(4S)	1.581(35)

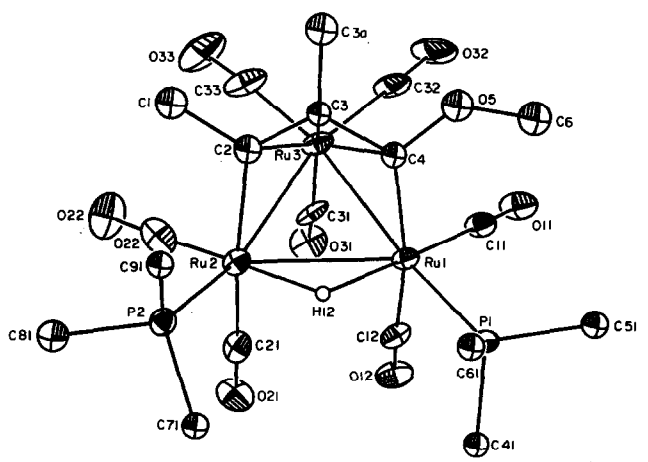

Fig. 4. Molecular core of $(\mu\text{-H})Ru_3(\mu_3\text{-}\eta^3\text{-MeOCCMeCMe})(CO)_7(PPh_3)_2$.

Å in the parent compound, $(\mu\text{-H})Ru_3(\mu_3\text{-}\eta^3\text{-MeOC-CMeCMe})(CO)_9$ [2]).

(4) As shown in Fig. 4, the two PPh_3 ligands occupy equatorial sites adjacent to the bridging hydride ligand, such that Ru(1)–P(1) = 2.361(4) Å and Ru(2)–P(2) = 2.346(4) Å, with associated angles of Ru(2)–Ru(1)–P(1) = 119.9(1)° and Ru(1)–Ru(2)–P(2) = 120.2(1)°.

4. Conclusion

(1) Substituted products $(\mu\text{-H})Ru_3(\mu_3\text{-}\eta^3\text{-XCCR-CR'})(CO)_{9-n}(PPh_3)_n$, $n = 1$–3, contain not more than one PPh_3 ligand per metal atom with the first and second substitutions occurring in coordination sites *cis* to both the bridging hydride and the sigma Ru–C bonds. Substitution *cis* to bridging hydride ligands has been shown to be favored on steric grounds [14].

(2) The use of trimethylamine-*N*-oxide to induce substitution at room temperature allowed us in one case to prepare a mixture of three isomers of $HRu_3(\mu_3\text{-}\eta^3\text{-MeOCCHCOEt})(CO)_7(PPh_3)_2$, including the two isomers in which one PPh_3 ligand is on the Ru atom η^3-bonded to the C_3 unit. These isomers rearrange slowly at room temperature to the thermodynamically stable product substituted on the Ru atoms sigma bonded to the 1- and 3-carbons of the allyl unit. This observation shows that the products derived from the thermally induced substitution on these clusters may not indicate the site of initial ligand substitution. At this time, the mechanism of isomerization has not been investigated.

(3) Although phosphine substitution for carbonyls in many clusters results in substantial changes in bond angles because of steric bulk of the phosphine ligand, the structure of $(\mu\text{-H})Ru_3(\mu_3\text{-}\eta^3\text{-MeOCCMeCMe})(CO)_7(PPh_3)_2$ and $(\mu\text{-H})Ru_3(\mu_3\text{-}\eta^3\text{-Et}_2\text{NCCHCMe})(CO)_8(PPh_3)$ show no significant distortions from the structures of the parent carbonyls. Therefore, differences in chemistry of $(\mu\text{-H})Ru_3(\mu_3\text{-}\eta^3\text{-XCCRCR'})(CO)_{9-n}(PPh_3)_n$ for different values of n may be safely ascribed to electronic effects.

(4) Our previous study [2] found that the Ru_3C_3 core geometry was very sensitive to the pi donor ability of carbon substituents, distorting from a *nido* structure based upon a pentagonal bipyramid toward an arachno structure. This work shows that the core geometry is quite insensitive to the replacement of π-acceptor CO ligands by σ-donor PPh_3 ligands.

5. Supplementary material available

Tables of observed and calculated structure factor amplitudes, interatomic angles, anisotropic thermal parameters and calculated positions of hydrogen atom for

$(\mu\text{-H})Ru_3(\mu_3\text{-}\eta^3\text{-}Et_2NCCHCMe)(CO)_8(PPh_3)$ and $(\mu\text{-H})Ru_3(\mu_3\text{-}\eta^3\text{-MeOCCMeCMe})(CO)_7(PPh_3)_2 \cdot 2CH_2Cl_2$ are available on request from M.R.C.

Acknowledgements

This work was supported by Grant CHE 89-00921 from the National Science Foundation. Purchase of the Siemens R3m/V diffractometer was made possible by Grant No. 89-13733 from the Chemical Instrumentation Program of the National Science Foundation.

References

1 Selected references: (a) M. Castiglioni, L. Milone, D. Osella, G.A. Vaglio and M. Valle, *Inorg. Chem., 15* (1976) 394; (b) G. Ganozzi, E. Tondello, R. Bertoncello, S. Aime and D. Osella, *Inorg. Chem., 24* (1985) 570; (c) B.E. Hanson, B.F.G. Johnson, J. Lewis and P.R. Raithby, *J. Chem. Soc., Dalton Trans.*, (1980) 1852; (d) J.W. Ziller, D.K. Bower, D.M. Dalton, J.B. Keister and M.R. Churchill, *Organometallics, 8* (1989) 492.

2 M.R. Churchill, L.A. Buttrey, J.B. Keister, J.W. Ziller, T.S. Janik, and W.S. Striejewske, *Organometallics, 9* (1990) 766.

3 (a) C. Jangala, E. Rosenberg, D. Skinner, S. Aime, L. Milone and E. Sappa, *Inorg. Chem., 19* (1980) 1571; (b) S. Aime, R. Gobetto, D. Osella, L. Milone and E. Rosenberg, *Organometallics, 1* (1982) 640.

4 L.R. Beanan and J.B. Keister, *Organometallics, 4* (1985) 1713.

5 (a) S. Aime, G. Jannon, D. Osella, A.J. Arce and A.J. Deeming, *J. Chem. Soc., Dalton Trans.*, (1984) 1987; (b) S. Aime, G. Jannon, D. Osella and A.J. Deeming, *J. Organomet. Chem., 114* (1981) C15.

6 S. Aime, D. Osella, A.J. Deeming, A.J. Arce, M.B. Hursthouse and H.M. Dawes, *J. Chem. Soc., Dalton Trans.*, (1986) 1459.

7 M.R. Churchill, R.A. Lashewycz and F.J. Rotella, *Inorg. Chem., 16* (1977) 265.

8 W. Nowacki, T. Matsumoto and A. Edenharter, *Acta Crystallogr., 22* (1967) 935.

9 SHELXTL PLUS Manual, 2nd Edition, Siemens Analytical X-Ray Instruments, Inc., 1990.

10 M.R. Churchill, *Inorg. Chem., 12* (1973) 1213.

11 M.O. Albers and N.J. Coville, *Coord. Chem. Rev., 53* (1984) 227.

12 M.R. Churchill, F.J. Hollander and J.P. Hutchinson, *Inorg. Chem., 10* (1977) 2655.

13 M.R. Churchill, C.H. Lake, W.G. Feighery and J.B. Keister, *Organometallics, 10* (1991) 2384.

14 (a) L.J. Farrugia, M. Green, D.R. Hankey, M. Murray, A.G. Orpen and F.G.A. Stone, *J. Chem. Soc., Dalton Trans.*, (1985) 177; (b) A.J. Deeming, S. Donovan-Mtunzi, S.E. Kabir, M.B. Hursthouse, K.M.A. Malik and N.P.C. Walker, *J. Chem. Soc., Dalton Trans.*, (1987) 1869.